Multi-Wavelength Optical Code Division Multiplexing

C. F. Lam and E. Yablonovitch
Electrical Engineering Department, UCLA, 405 Hilgard Ave., Los Angeles, CA 90095-1594, USA

1. Introduction

In the past 10 or 15 years there has been tremendous interest in applying spread spectrum and code division multiple access (CDMA) concepts to optical communications. CDMA has been successfully deployed in military systems for secure communications and cellular phone systems to make efficient use of the radio spectrum. Among the advantages of CDMA systems are their anti-jamming capability, low probability of detection, and inherent security advantage due to spread spectrum encoding. However, for more general communications purposes, most optical CDMA schemes were not competitive, in terms of system throughput and capacity, with more conventional schemes like wavelength division multiplexing (WDM). Here we describe a multi-wavelength spectrally encoded optical CDMA system that begins to approach WDM performance.

In a CDMA system,[1,2] the signal is spread over a much wider channel than required for data transmission. Each channel consists of a spread spectrum code signature and is broadcast to all receivers on the same network. The code signature is removed at the receiver by auto-correlation with a matched code. Different channels are encoded with signatures orthogonal to one another and unmatched code signatures are rejected. The receiver needs the correct code in order to recover the signal, which leads to enhanced security.

In an optical CDMA system, encoding and decoding are performed in the optical domain. In fact, optical CDMA was first conceived as a multiple access protocol in an optical local area network (LAN) environment, by making use of the tremendous bandwidth available in the optical fiber, thereby avoiding the electronic processing bottleneck.[3,4]

Different approaches have been proposed for optical CDMA systems. Electrical field detection is widely used in radio systems while intensity detection is more popular in optical systems due to the difficulties in phase locking and polarization maintenance of optical signals. Since electrical fields are bipolar in nature, spreading code signatures with both positive and negative components can lead to true orthogonality,[1,2] which is vital for avoiding cross-talk. Positive-only intensity detection schemes, used in most optical communication systems, make code orthogonality and cross-channel cancellation more difficult to achieve.

One example of optical CDMA uses an optical delay-line network to transform an ultra-short optical pulse into a train of low intensity pulses occupying

Future Trends in Microelectronics, Edited by S. Luryi, J. Xu, and A. Zaslavsky.
ISBN 0-471-32183-4

a bit period.[3-6] A conjugate delay-line network is used at the receiver to reconstruct the original short pulse. Orthogonality is impossible in such systems. In order to reduce the crosstalk, codes with long length and small weight are used, which leads to inefficient use of the available spectrum. Code families used in such systems include optical orthogonal codes,[7] prime sequence codes,[8] *etc.* The non-zero cross-correlation of these codes severely limits the bit error rate (BER).

Other approaches to optical CDMA involve frequency domain processing by spectral encoding. A dispersive element is used to decompose the frequency components in a broadband optical signal. The coherent approach[9,10] uses pseudo-random phase encoding of the spectral components to disperse a sharp narrow spike in the time domain into a broad noise-like low intensity signal. The sharp spike is reconstructed by conjugate phase encoding of the received signal. A non-linear threshold device is used to differentiate between a reconstructed high intensity narrow spike and unmatched low-intensity background interference signal. This approach is very sensitive to phase shifts in the fiber channel. The non-linear detection scheme is also clumsy and cumbersome.

A non-coherent spectral intensity encoding approach has also been proposed and demonstrated.[11,12] In this approach, the transmitter selectively transmits certain wavelength components for each channel. The receiver uses a pair of complementary spectral filters and balanced detectors to cancel unmatched spectra and transmit the desired spectrum. Bipolar signaling and full orthogonality can be achieved in spite of the absence of a coherent local oscillator. Unfortunately, the BER of this system and most other optical CDMA systems is limited by the speckle noise generated due to the interference of optical waves of the same wavelength coming from different transmitters.

In this paper, we describe a novel optical CDMA approach that uses phase encoding of a mode-locked laser to create pseudo-random noise patterns. These patterns can be regarded as a carrier transmitted along with modulation side-bands. At the receiver, this encoded carrier is mixed with the encoded modulation side-bands in a double balanced mixer to recover the information. The ultimate performance of this system is shot noise limited, and is analyzed in this paper.

2. Transmitter

A multi-wavelength optical CDMA network architecture is shown in Fig. 1. Each user broadcasts its optically encoded signal to all other users in the network through a star coupler. The mode-locked laser pulses of each user synchronize with the rest of the network through a time synchronization signal generated by the receiver which monitors the star coupler. The pulses should arrive at the star coupler simultaneously from all transmitters. Absolute optical phase synchronization is not needed.

Figure 2 shows the block diagram of the transmitter which uses a mode-locked laser as the optical source.[13] The output of the mode-locked laser source

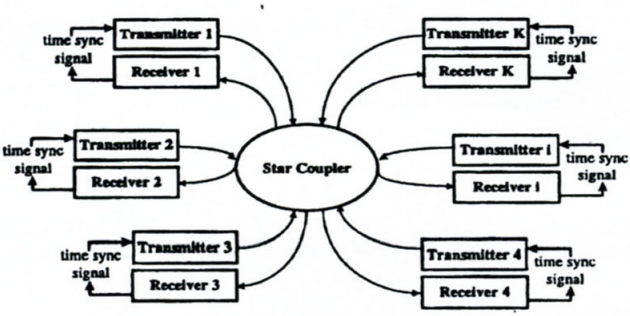

Figure 1. Schematic CDMA network architecture.

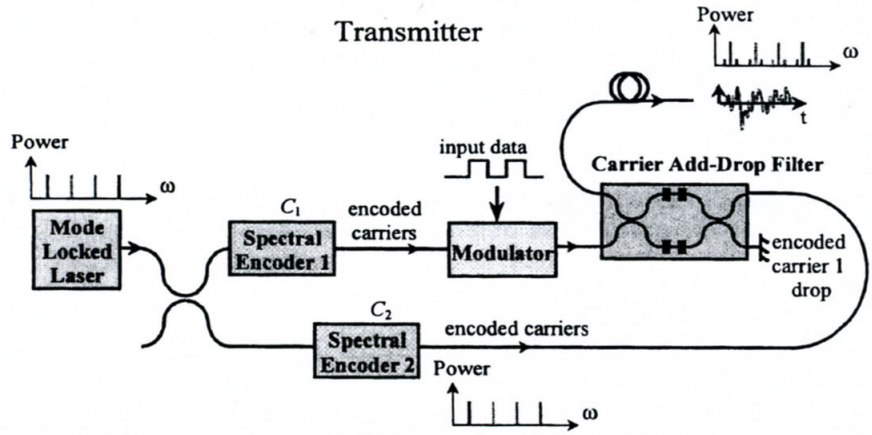

Figure 2. The transmitter provides both encoded side-bands C_1 and a separately encoded carrier C_2.

can be represented by:

$$E(t) = E_0 \exp(i\omega t) \sum_{n=0}^{N-1} \frac{1}{\sqrt{N}} \exp[in(\Delta\omega)t] \tag{1}$$

where $\Delta\omega/2\pi$ is the pulse repetition frequency.

There are several good reasons to use a mode-locked laser. First, the multiple harmonics of a mode-locked laser are phase-synchronized with respect to each other. They provide the vector space for encoding and are broadband as needed for spread-spectrum CDMA systems. Second, because the phases of the spectral components are locked with respect to each other, the output from a mode-locked laser consists of pulse trains separated by $T = 2\pi/\Delta\omega$. These well defined pulses can be used to synchronize each user with respect to other users. Third, because of the well-defined phase relationships between different spectral components, we

can apply phase encoding to ensure perfectly orthogonal codes, as opposed to other optical CDMA systems which use intensity encoding in the time domain. At the same time, we do not have to track the absolute optical phase, but only the relative phase shift between different mode-locked frequency components.

The mode-locked laser output forms the carrier for the signal. It is split into two halves using a 3-dB splitter. We define the encoding operation $C_k[E(t)]$ for encoder k as:

$$C_k[E(t)] = C_k(t) = E_0 \exp(i\omega t) \sum_{n=0}^{N-1} \frac{1}{\sqrt{N}} \exp\left\{ i n(\Delta\omega)t + \Phi_{kn} \right\} \tag{2}$$

where Φ_{kn} is the encoded phase on the nth spectral component. The codes are designed to be orthogonal so that two codes C_k and C_h satisfy:

$$C_k \bullet C_h^* = E_0^2 \sum_{n=0}^{N-1} \frac{1}{N} \exp\left\{ i(\Phi_{kn} - \Phi_{hn}) \right\} = E_0^2 \delta_{kh} \tag{3}$$

where $\delta_{kh} = 1$ if $k = h$ and 0 otherwise. In the simplest case, if we use 0's and π's as the encoded phase shifts, the codes correspond to multiplication coefficients of +1 and −1 in the frequency domain. All the good bipolar codes developed for radio CDMA can be directly applied to our system including, for example, the Hadamard codes[14] that form the rows of a Hadamard square matrix. Two codes are orthogonal when the phase differences between the corresponding spectral components are given by $\exp[i(\Phi_{kn} - \Phi_{hn})]$ and are uniformly distributed on a unit circle in a complex plane. A new encoder family using cascaded feedback Mach-Zehnder interferometers will be introduced in the latter part of this paper.

For the kth user, the first half of the carrier passes through a spectral filter which phase encodes the carrier components as:

$$C_{k,1}(t) = \frac{1}{\sqrt{2}} E_0 \exp(i\omega t) \sum_{n=0}^{N-1} \frac{1}{\sqrt{N}} \exp\left\{ i[n(\Delta\omega)t + \Phi_{kn,1}] \right\} \tag{4}$$

The other half of the spectral components of the kth user are encoded by a different code $C_{k,2}$ in a similar way:

$$C_{k,2}(t) = \frac{1}{\sqrt{2}} E_0 \exp(i\omega t) \sum_{n=0}^{N-1} \frac{1}{\sqrt{N}} \exp\left\{ i[n(\Delta\omega)t + \Phi_{kn,2}] \right\} \tag{5}$$

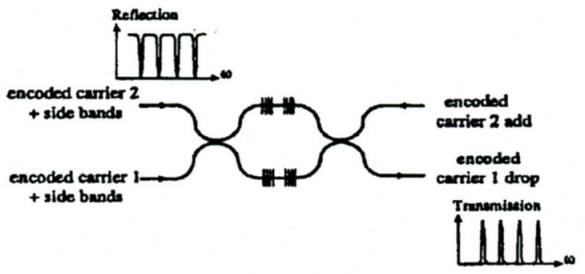

Figure 3.

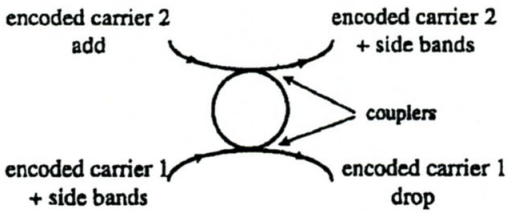

Figure 4.

The power spectral density function of the encoded carrier still looks the same as that of the unencoded carrier in the frequency domain. However, in the time domain, it resembles a pseudo-random noise pattern.

A modulator is placed after the encoded carrier $C_{k,1}$ to impose data modulation. Either phase or intensity modulation could be applied. The modulated output is:

$$X_k(t) = s_k(t)C_{k,1}(t) \tag{6}$$

where $s_k(t)$ is the data signal for the kth user. For amplitude shift keying (ASK) $s_k(t) = 0$ or $+1$, while for phase shift keying (PSK), $s_k(t) = +1$ or -1. Modulation generates the information-containing side bands $s_k(t)C_{k,1}(t)$ around the pure carrier tones $C_{k,1}(t)$. This signal is passed through a carrier add-drop filter consisting of a balanced Mach-Zehnder interferometer (MZI) with a pair of identical high-finesse Fabry-Perot (FP) filters in both arms. The FP filters have very sharp frequency transmission at the carrier tone frequencies and very high reflection for frequencies other than the carrier tones (Fig. 3). The residual encoded carrier tones $C_{k,1}(t)$ will pass through the MZI and will be dropped at the carrier drop port on the opposite side of the input signal. The information-containing side bands will be reflected to the other port on the same side of the signal.

The transmitter also adds the encoded carrier $C_{k,2}(t)$ to the reflected side bands from the carrier add port of the MZI. The added carrier will be extracted at the receiver as the "local oscillator" to demodulate the transmitted signal. A similar MZI arrangement for carrier add/drop filters has been used with fiber gratings as a wavelength division multiple-access (WDM) add/drop multiplexer.[15] Another possible carrier add/drop filter consists of a ring coupler pair shown in Fig. 4. This filter is made up of two weak couplers connected in a ring whose size matches the resonant condition for the carrier tones. The carriers will be coupled out of the carrier drop port because of resonance. The device can be made very compact and has the potential for integrated photonics.[16]

3. Receiver

The side bands and the encoded carrier are broadcast to the receivers through a star coupler. Figure 5 shows the receiver structure. The same carrier add-drop filter is

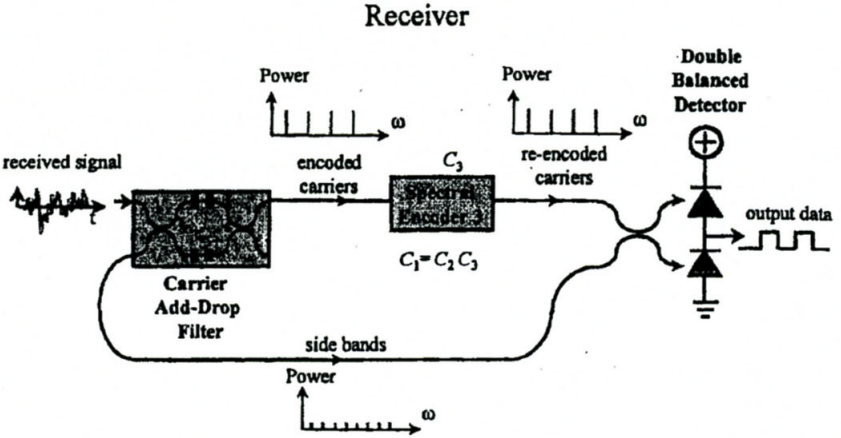

Figure 5.

used to separate the side bands and the encoded carrier tones. The carrier tones go through another spectral encoder C_3 at the receiver such that $C_{k,1} = C_{k,3}C_{k,2}$ and $C_{k,1}$ is orthogonal to $C_{k,3}C_{j,2}$ for $j \neq k$. Thus the receiver reconstructs the encoded carrier $C_{k,1}$. The side bands and the reconstructed carriers beat at a second 3-dB splitter which is part of a double balanced detector.

Without loss of generality, let $k = 1$ be the desired channel. The input to the second beam splitter consists of the multiplexed side bands and the re-encoded carriers The outputs consist of the sum $R_{U1}(t)$ and difference $R_{L1}(t)$ of the side bands and the encoded carrier of the desired user, i.e. user 1:

$$R_{U1}(t) = \frac{1}{\sqrt{2}} \sum_{k=1}^{K} s_k(t) C_{k,1}(t) + \frac{1}{\sqrt{2}} C_{1,3} \sum_{k=1}^{K} C_{k,2}(t) \tag{7}$$

$$R_{L1}(t) = \frac{1}{\sqrt{2}} \sum_{k=1}^{K} s_k(t_k) C_{k,1}(t) - \frac{1}{\sqrt{2}} C_{1,3} \sum_{k=1}^{K} C_{k,2}(t) \tag{8}$$

The photodetectors used in the balanced receiver can be considered a pair of square law devices followed by a low pass filter. Therefore, the output from the balanced detector will be:

$$\begin{aligned} Z_1(t) &= \mathrm{LP}\left[\frac{\Re}{2}\left|R_{U1}(t)\right|^2 - \frac{\Re}{2}\left|R_{L1}(t)\right|^2\right] \\ &= \mathrm{LP}\left[\frac{\Re}{2}\left(\sum_{k=1}^{K} s_k(t) C_{k,1}(t)\right) \bullet \left(C_{1,3} \sum_{k=1}^{K} C_{k,2}(t)\right)^*\right] \end{aligned} \tag{9}$$

where $\Re$ is the responsivity of the photodetectors. The square terms of the side bands and re-encoded carrier tones are cancelled at the balanced detector output, eliminating any common mode fluctuations. The remaining term is the low-pass filtered cross product between the side bands and the re-encoded carriers. By the

code orthogonality requirement, all the dot product terms are cancelled except for user 1. The operation of $C_{1,3}$ on $C_{1,2}$ regenerates $C_{1,1}$ — the correct "local oscillator" used to extract the user 1 signal $s_1(t)$. By maintaining mode-locked time synchronization, perfect orthogonality can be achieved.

4. Decoder

In this section, we describe the design of an encoder that uses series-connected MZIs. The MZIs are set in a feedback configuration as shown in Fig. 6. The output of the feedback MZI (FBMZI) is determined by three parameters, the feed forward path length difference l_f between the two feed forward paths, the extra phase θ introduced by a phase shifter at the second arm of the MZI and the feedback delay introduced by the feedback path l_b. A general frequency transfer function for an arbitrary FBMZI can be easily derived using feedback network theory. Here, we describe a specific design that will generate orthogonal codes.

We assume N, the total number of frequency components in the mode-locked laser spectrum, to be a power of 2, i.e. $N = 2^L$, where L is an integer. The feed forward path length difference l_f and the feedback path length l_b can be expressed by the corresponding time delays $\tau_f = l_f/c$ and $\tau_b = l_b/c$, where c is the speed of light in the waveguide. For simplicity, we restrict the values of τ_f and τ_b to integral multiples of a basic time unit $\tau_0 = 2\pi/(N\Delta\omega)$, which is the reciprocal of the total CDMA bandwidth. In addition, let us restrict the phase shift θ to either 0 or π.

It can be easily shown[17] that setting the feed forward path difference delay to be $\tau_f = N\tau_0/2 = \pi/\Delta\omega$ corresponds to an MZI whose free spectral range (FSR) is $2\Delta\omega$. We can view the MZI as a 2×2 switch for the frequency components that

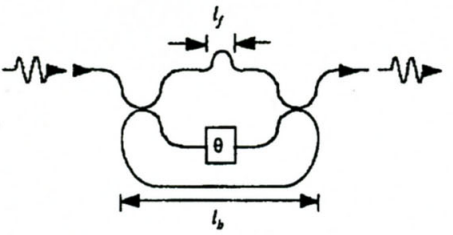

Figure 6.

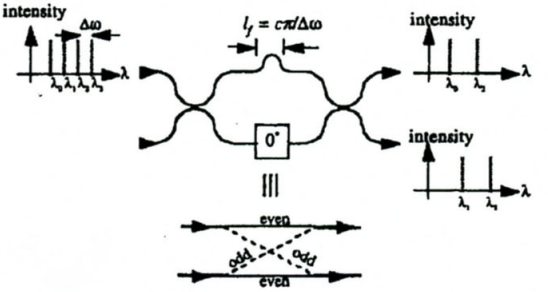

Figure 7.

are separated by $\Delta\omega$. Half of the frequency components (say the even ones) will see the MZI in the through state and the other half (the odd components) will see the MZI in the cross state (Fig. 7). When a phase shift $\theta = \pi$ is introduced at the MZI, the roles of the frequency components are changed so that the ones previously in the through state are now in the cross state and vice versa.

Components in the cross state are fed back to the other input port of the MZI and come out of the same output port as those in the through state after a feedback delay τ_b, which is translated into a phase shift. The 0 and π phase shifts in the feed forward path represent two binary states of an encoder.

Let the feedback delay be $\tau_b = q\tau_0$, where q is an integer. Because of limited space, we will state the following theorems without proof.

- *Theorem 1.* If q and N are co-prime (i.e. they have no common factor), the codes generated by the 0 and π states are orthogonal. The net phase differences for all the N frequency components are distributed on the complex unit circle without repetition.

The actual phase difference pattern is dependent on the value of q, which can be considered a cryptographic factor[18] for encoding. Figure 8 shows the encoded phase differences on the unit circle for $N = 32$ and $q = 1$, 3, and 7.

- *Theorem 2.* If q and N are not co-prime and have as their greatest common divisor (gcd) the integer 2^m, $m < L$, the codes produced by the 0 and π states are orthogonal within a free spectral range (FSR) of $(N\Delta\omega)/2^m$.

In other words, the encoded phase difference pattern will repeat for every $N/2^m$ frequency components and the orthogonality also covers every $N/2^m$ frequency components. For simplicity, we will say the normalized FSR of the encoder is $N/2^m$ later on. Of course, the orthogonality extends to all the N components. We can express q as $q=2^m r$ where r is an odd number that determines the actual locations of the frequency components on the complex plane. Figure 9 shows the distribution of the phase differences for $r = 3$ and 7, $N = 32$, and $m = 2$.

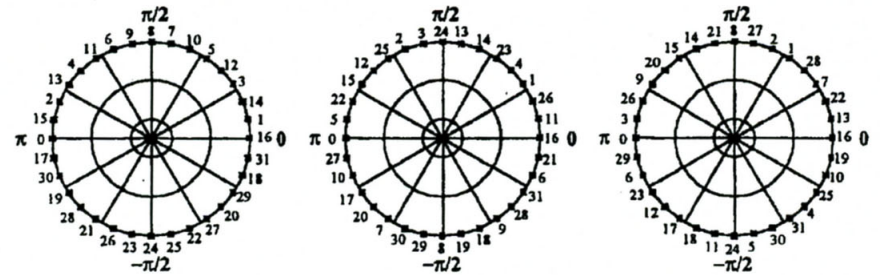

Figure 8. Distribution of the phase difference between two different states for an encoder with (a) $q = 1$, (b) $q = 3$ and (c) $q = 5$. $N = 32$ frequencies labeled from 0 to 31 are used for encoding.

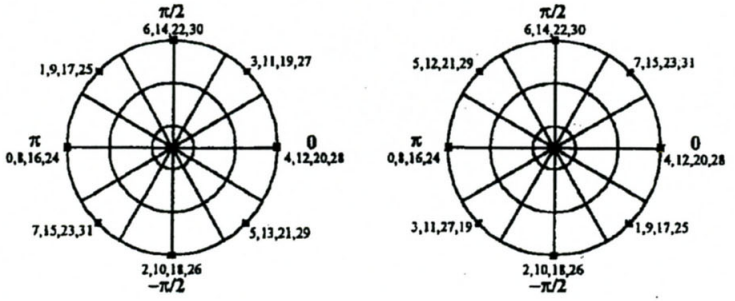

Figure 9. Distribution of the phase difference between two different states for an encoder with $q = 2^m r$ where $m = 2$ and (a) $r = 3$ and (b) $r = 7$. $N = 32$ frequencies labeled from 0 to 31 are used for encoding.

Theorems 1 and 2 together state that for all the integers q, the two states formed by the FBMZI encoder are orthogonal to each other. The next theorem states that a family of orthogonal codes can be generated by cascading encoders with different FSRs.

- *Theorem 3.* Suppose two FBMZIs have a normalized FSR of N and $N/2$ respectively. Each stage has two states 0 and π. The four possible states obtained by combining the two stages generate four mutually orthogonal codes.

Theorem 3 can be extended by induction to prove that by cascading a series of encoders with L different normalized FSRs (i.e. 2, 2^2, ..., 2^L) one can obtain all 2^L orthogonal codes. The 2^L codes are produced by different combinations of the 0 or π shifts in the various stages. One plausible way of cascading the FBMZIs is to use a waveguide design with "concentric" circles touching each other to form the 3-dB couplers. The waveguides are nested in cascade as shown in Fig. 10. The output waveguide cut the loops perpendicularly to eliminate the crosstalk.

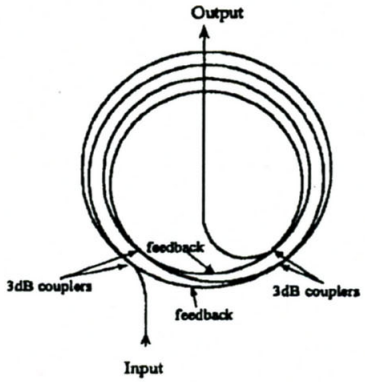

Figure 10.

5. Performance analysis

In this section, we investigate the performance limit of the proposed optical CDMA system. Again, we take user 1 as the intended channel. Assume the carriers $C_{k,1}$ and $C_{k,2}$ have the same amplitude. The value of $s_k(t)$ is 0 or 1 for ASK and −1 or +1 for PSK. Ideally, the carrier decoding by the $C_{k,3}$ does not change the amplitude of $C_{k,2}(t)$ because only phase encoding is used.

From Eqs. (4) and (5), we obtain that for each user the power in both carriers $P[C_{k,1}(t)]$ and $P[C_{k,2}(t)]$ is $E_0^2/4$. Assume 0 and 1 bits are equally probable. The average received power is:

$$P_{rec} = \alpha P[C_{k,1}(t)] + P[C_{k,2}(t)] = \frac{(\alpha+1)E_0^2}{4} \tag{10}$$

or $E_0 = [4P_{rec}/(\alpha + 1)]^{1/2}$, where $\alpha = 1/2$ for ASK and $\alpha = 1$ for PSK. Here we have assumed that the received power from all the users are equal. The splitting loss at the star coupler is also ignored.

The useful output signal is given by Eq. (9). Due to the code orthogonality, only the matched term corresponding to user 1 will survive. So we have:

$$\begin{aligned} Z_1(t) &= \mathrm{LP}\left[\frac{\Re}{2}\left(\sum_{k=1}^{K} s_k(t)C_{k,1}(t)\right)\bullet\left(C_{1,3}\left[\sum_{k=1}^{K} C_{k,2}(t)\right]\right)^*\right] \\ &= \mathrm{LP}\left[\frac{\Re}{2}\left(s_1(t)C_{1,1}(t)\right)\bullet\left(C_{1,3}[C_{1,2}(t)]\right)^*\right] \\ &= \mathrm{LP}\left[\frac{\Re}{2}\left(s_1(t)C_{1,1}(t)\right)\bullet\left(C_{1,1}(t)\right)^*\right] \\ &= \frac{\Re E_0^2}{4}s_1(t) = \frac{\Re P_{rec}}{\alpha+1}s_1(t) \end{aligned} \tag{11}$$

The average received signal (root mean square) is thus:

$$I_{sig} = \sqrt{\overline{Z_1(t)^2}} = \frac{\sqrt{\alpha}}{\alpha+1}\Re P_{rec} \tag{12}$$

The signals detected by each of the two photodetectors in the balanced receiver are given by $R_{U1}(t)$ and $R_{L1}(t)$ as in Eqs. (7) and (8). Since the received user power (both side bands and re-encoded carriers) is split equally by the 3dB splitter in front of the balanced detector, the average optical power seen by each photodetector is:

$$\frac{1}{2}\overline{|R_{U1}|^2} = \frac{1}{2}\overline{|R_{L1}|^2} = \frac{KP_{rec}}{2} \tag{13}$$

This detected optical power will contribute shot noise[17] at each photodetector. The shot noise produced is therefore:

$$\left\langle I_{sh}^2\right\rangle_{U1} = \left\langle I_{sh}^2\right\rangle_{L1} = 2qIB_d = q\Re KP_{rec}B_d \tag{14}$$

where $\Re$ is the responsivity of the photodetector, B_d is the data bandwidth and I is the average photocurrent produced at each photodetector. The total shot noise is thus:

$$\left\langle I_{sh}^2 \right\rangle = \left\langle I_{sh}^2 \right\rangle_{U1} + \left\langle I_{sh}^2 \right\rangle_{L1} = 2q\Re KP_{rec}B_d \tag{15}$$

We can see that co-channel users degrade the performance of the system by increasing the shot-noise proportionately. For a received power of –20 dB (10μW) per active user at a receiver bit rate of 1 Gbps, using $\Re$ = 0.8A/W for a typical InGaAs PIN photodiode working in the 1.5 μm wavelength range, the rms shot noise is 5.06×10^{-8} A for one user.

Another source of noise is the Gaussian-distributed thermal noise from the receiver pre-amp which is given by:

$$\left\langle I_{th}^2 \right\rangle = \frac{4kT}{R_L}B_d = 8\pi kTB_d^2C \tag{16}$$

where R_L is the receiver load resistance and $B_d = 1/T_b = 1/2\pi R_LC$ (T_b is the bit period and C is the load capacitance). For state-of-the-art technology, $C \approx 0.02$ pF. Using other parameter values as before, the rms thermal noise is 4.57×10^{-8} A.

It is worth noting that all signals are split equally between the two photo-detectors in the balanced detector, so the common-mode fluctuations in the signal and carrier power are cancelled by the balanced detector, except for the shot noise. Since shot noise and thermal noise arise from independent mechanisms, the total mean square noise $\langle I_n^2 \rangle$ is their sum.

The bit error rate (BER) for ASK is given by:[19]

$$BER = \frac{1}{2}\left[1 - erf\left(\sqrt{\frac{\gamma E_b}{2N_0}}\right)\right] \tag{17}$$

where E_b is the average bit energy, γ= 1 for ASK and γ= 2 for PSK, and N_0 is the two sided noise power spectral density. One then obtains:

$$\frac{E_b}{N_0} = \frac{I_{sig}^2T_b}{N_0} = \frac{I_{sig}^2}{N_0B_d} = \frac{I_{sig}^2}{\left\langle I_n^2 \right\rangle} \tag{18}$$

Figure 11 plots the BER against the number of co-channel users at various received power levels for PSK (a 1 Gbps data rate is assumed for each user). It is seen from Fig. 11 that for –20 dBm received power per channel, 197 and 346 concurrent users are allowed for a BER of 10^{-15} and 10^{-9} respectively.

It is also worth noting that this is the worst-case situation. For a system with bursty traffic, the number of concurrent users will likely to be much less than the total number of subscribers. From the above analysis, the SNR is shot-noise limited when the total received power $P_{rec}K$ is large and is approximately:

$$SNR \approx \frac{I_{sig}^2}{\left\langle I_{sh}^2 \right\rangle} = \frac{\alpha\Re P_{rec}}{2q(\alpha+1)^2KB_d} \tag{19}$$

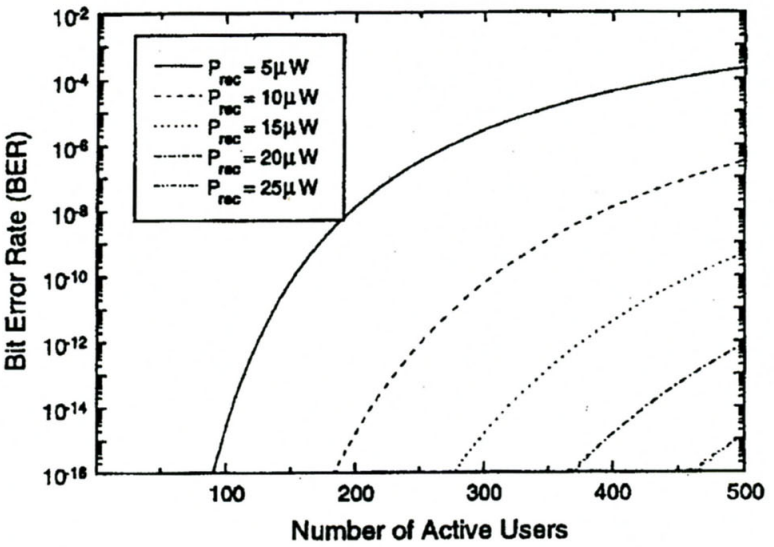

Figure 11. BER *vs.* number of active users for PSK.

The total network throughput is given by KB_d. The network throughput scales linearly as the received power per channel increases.

From the transmitter's point of view, the signal is broadcast to all the users in the network by a passive optical star coupler. Suppose the network size is the same as the total number of active users (the most pessimistic case). Then the splitting loss is 10log$K$ dB. Neglecting the transmission loss and other non-idealities, the signal to noise ratio in terms of the transmitter power P_t is given by:

$$SNR \approx \frac{I_{sig}^2}{\langle I_{sh}^2 \rangle} = \frac{\alpha \Re P_t}{2q(\alpha+1)^2 K^2 B_d} \tag{20}$$

The total throughput is given by:

$$KB_d \approx \frac{\alpha \Re P_t}{2q(\alpha+1)K \cdot SNR} \tag{21}$$

For a given available transmitter power, to obtain higher throughput, the total number of users needs to be smaller, which also means that each channel needs to handle a bigger bandwidth. Assuming 10 mW available optical power at the transmitter output and 150 concurrent users, the network can support a total capacity of 2.3 THz for PSK at 10^{-9} BER. Figure 12 plots the achievable throughput for different values of P_t. The transmitter power is assumed to be evenly distributed among all the subscribers who are all active at the same time (again the worst case).

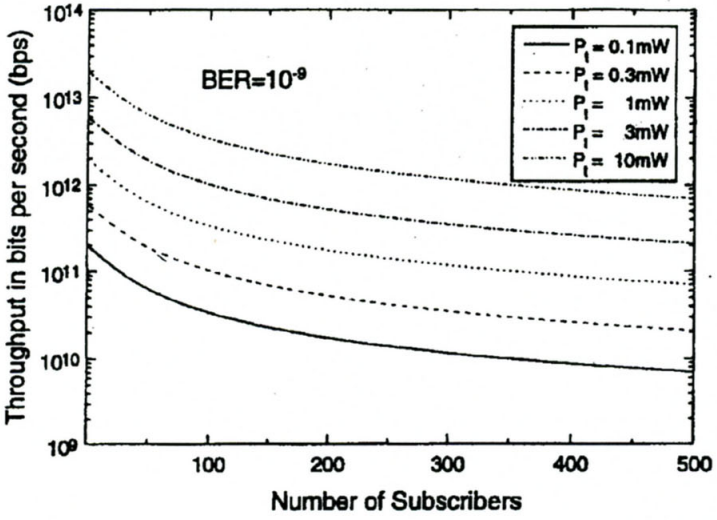

Figure 12. Throughput *vs.* number of subscribers for PSK.

6. Discussion and conclusion

In the proposed system, we have inserted a separately encoded carrier with the modulated signal for transmission. This transmitted carrier is separated from the information bearing side bands at the receiver and is used to reconstruct the code that is applied to the information-bearing carrier. This separately encoded carrier serves as an externally supplied local oscillator at the receiver, eliminates the requirement of a separate local oscillator, and helps to reduce the system cost. Since the encoded pure carrier and the side bands are generated from the same source and they travel through the same network to the receiver, there is no complicated phase locked loop mechanism required for phase synchronization of the local oscillator. The idea is stimulated by amplitude modulated (AM) radio communication systems. The output spectrum of an AM signal consists of side bands and the carrier tone. The envelope detector in an AM receiver mixes the side bands with the carrier tone, which functions as an externally supplied local oscillator in exactly the same fashion as our balanced photodetectors.

The codes applied to the pure carrier and the sides bands are orthogonal to each other so that simple square law detection will not give any output, protecting the signal from being intercepted by the unwanted receivers and enhancing the system security. As an alternative, one could conceive transmitting the unencoded carrier, which is produced by the mode-locked laser, to reconstruct the code used on the side bands. Since each user broadcasts its signal to all the users in the network, different copies of the unencoded carrier will add non-coherently at the receiver and fluctuate in intensity. This fluctuation is due to the difficulty of synchronizing the absolute phase of the optical carrier. The reconstructed code

will therefore fluctuate in the same way as the laser speckle noise. The beating of this noisy code with the side bands will give excess fluctuations in the output signal. Thus, by encoding the pure carriers in each channel with a different code, only the desired encoded carrier will detect the desired side bands. The carrier from all other channels will carry orthogonal codes.

Time synchronization of mode-locked pulses is required, however, and has been researched in studies of high-speed optical TDMA systems. The synchronization techniques used in those systems could be applicable to our CDMA system. There are two methods to maintain time synchronization among the transmitters. In the first approach, a high performance mode-locked laser source may be shared across the network by distributing its outputs to various users using the star coupler. Since the cost of the high performance source is shared among different users, the average cost could still be reasonable. In the second approach, a master reference laser can be used to synchronize the individual sources through the star coupler.

We have seen that the balanced receiver used in this paper has the ability to reject the common-mode fluctuation in the signal sources and achieve true orthogonality. Eventually, the system will be shot noise limited when the number of users accessing the network is large. When the system is shot noise limited, increasing the signal power improves the BER by increasing the SNR. However, when a system is speckle noise limited as in a non-coherent spectral intensity encoded system,[11,12] the SNR does not improve by increasing the signal power and the system performance is very limited.

In conclusion, we have proposed an optical CDMA system that is able to achieve full orthogonality and shot noise limited performance. An encoder structure based on feedback Mach-Zehnder interferometers has been proposed. The performance analysis suggests an achievable throughput of 1Tbit/s.

References

1. R. L. Pickholtz, D. L. Schilling, and L. Milstein, "Theory of spread spectrum communications — a tutorial," *IEEE Trans. Commun.* **30**, 855 (1982).
2. R. L. Peterson, R. E. Ziemer, and D. E. Borth, *Introduction to Spread Spectrum Communications*, Englewood Cliffs, NJ: Prentice Hall, 1995.
3. J. Y. Hui, "Pattern code modulation and optical decoding — a novel code-division multiplexing technique for multifiber networks", *IEEE J. Selected Areas Commun.* **3**, 916 (1985).
4. P. R. Prucnal, M. A. Santoro, and T. Fan, "Spread spectrum fiber-optic local area network using optical processing," *J. Lightwave Technol.* **4**, 547 (1986).
5. P. R. Prucnal, M. A. Santoro, and S. K. Sehgal, "Ultrafast all-optical synchronous multiple access fiber optical networks," *IEEE J. Selected Areas Commun.* **4**, 1484 (1986).

6. J. A. Salehi, "Code division multiple-access techniques in optical fiber networks — part I: fundamental principles," *IEEE Trans. Commun.* **37**, 824 (1989).
7. F. R. K. Chung, J. A. Salehi, and V. K. Wei, "Optical orthogonal codes: design, analysis and applications," *IEEE Trans. Info. Theory* **35**, 595 (1989).
8. L. Tanccevski and I. Andonovic, "Hybrid wavelength hopping/time spreading schemes for use in massive optical networks with increased security," *J. Lightwave Technol.* **14**, 2636 (1996).
9. J. A. Salehi, A. M. Weiner, and J. P. Heritage, "Coherent ultrashort light pulse code-division multiple access communication systems", *J. Lightwave Technol.* **8**, 478 (1990).
10. C. C. Chang, H. P. Sardesai, and A. M. Weiner, "Code-division multiple-access encoding and decoding of femtosecond optical pulses over a 2.5-km fiber link," *IEEE Photonics Technol. Lett.* **10**, 171 (1998).
11. M. Kvehrad and D. Zaccarin, "Optical code-division-multiplexed systems based on spectral encoding of noncoherent sources", *J. Lightwave Technol.* **13**, 534 (1995);
    L. Nguyen, T. Dennis, B. Aazhang, and J. F. Young, "Optical spectral amplitude CDMA communication," *J. Lightwave Technol.* **15**, 1647 (1997).
12. C. F. Lam, D. T. K. Tong, M. C. Wu, and E. Yablonovitch, "Experimental demonstration of bipolar optical CDMA system using a balanced transmitter and complementary spectral encoding," *IEEE Photonics Technol. Lett.* **10**, 1504 (1998).
13. Y. K. Chen and M. C. Wu, "Monolithic colliding pulse mode-locked quantum well lasers," *IEEE J. Quantum Electronics* **28**, 2176 (1992).
14. A. K. Jain, *Fundamentals of Digital Image Processing*, Englewood Cliffs, NJ: Prentice Hall, 1986.
15. F. Bilodeau, D. C. Johnson, S. Theriault, *et al.*, "An all-fiber dense-wavelength-division multiplexer/demultiplexer using photoimprinted Bragg gratings," *IEEE Photonics Technol. Lett.* **7**, 388 (1995).
16. B. E. Little, J. S. Foresi, G. Steinmeyer, *et al.*, "Ultra-compact Si-SiO_2 microring resonator optical channel dropping filters," *IEEE Photonics Technol. Lett.* **10**, 549 (1998).
17. P. E. Green, Jr., *Fiber Optic Networks*, Englewood Cliffs, NJ: Prentice-Hall, 1993.
18. N. Koblitz, *A Course in Number Theory and Cryptography*, 2nd ed., New York: Springer-Verlag, 1948.
19. R. E. Ziemer and R. L. Peterson, *Introduction to Digital Communication*, New York: Macmillan, 1992.